American Journal of Applied Mathematics and Statistics, 2015, Vol. 3, No. 6, 211-219
Available online at http://pubs.sciepub.com/ajams/3/6/1

DOI:10.12691/ajams-3-6-1

Boundary Layer Stagnation-Point Flow of Second Grade Fluid over an Exponentially Stretching Sheet

Abdul Rehman[1,*], Ghulam Farooq[1], Israr Ahmed[1], Muhammad Naseer[2], Muhammad Zulfiqar[3]

[1]Department of Mathematics, University of Balochistan, Quetta, Pakistan
[2]Department of Mathematics, Quaid-i-Azam University, Islamabad, Pakistan
[3]Department of Mathematics, GC University, Lahore, Pakistan
*Corresponding author: rehman_maths@hotmail.com

Abstract In this paper, the steady boundary layer stagnation point flow and heat transfer of a second grade fluid over an exponentially stretching sheet is investigated. The solutions are obtained through homotopy analysis method (HAM) and the Keller-box technique. Comparisons of both the solutions are given graphically as well as in tabular form. The effects of second grade parameter β, Prandtl number Pr, and other important physical parameters are presented through graphs and the salient features are discussed.

Keywords: *boundary layer flow, heat transfer, second grade fluid, exponential stretching/shrinking, homotopy analysis method, keller-box technique*

Cite This Article: Abdul Rehman, Ghulam Farooq, Israr Ahmed, Muhammad Naseer, and Muhammad Zulfiqar, "Boundary Layer Stagnation-Point Flow of Second Grade Fluid over an Exponentially Stretching Sheet." *American Journal of Applied Mathematics and Statistics*, vol. 3, no. 6 (2015): 211-219. doi: 10.12691/ajams-3-6-1.

1. Introduction

Boundary layer flow due to stretching and stagnation point flows have achieved considerable attention due to its applications in industry and manufacturing processes. A large number of researchers are engaged with this area. Mention may be made to the works of [1-15]. In the analysis mentioned above simple stretching and stagnation flow have been used. However some researchers have used the exponential stretching because of its engineering applications. Sanjayanad and Khan [16] and Khan and Sanjayanad [17] have discussed the boundary layer flow of viscoelastic fluid due to exponential stretching sheet with and without heat transfer analysis. Later on, the idea of exponential stretching have further discussed by Nadeem et al [18,19] for considering different non-Newtonian fluid models. Recently, Wei et al [20] have considered the stagnation point flow over an exponentially stretching/shrinking sheet for the viscous fluids.

Motivated from the above analysis, the aim of the present paper is to discuss the boundary layer flow of second grade fluid over an exponential stretching sheet. To the best of author's knowledge only a single attempt is available which discussed the exponential stagnation with the exponential stretching when fluid is taken as Newtonian. However, this analysis has not been discussed so far for non-Newtonian fluids. Therefore, in this paper we have discussed both the analytical and numerical solutions of the second grade fluid with exponential stagnation point flow with exponential stretching in the presence of mixed convection heat transfer. It is also worth able to mention here that we have discussed the two strong solution techniques together. The analytical solutions are carried out with the help of homotopy analysis method [21-28]. For validity of the solution we have also provided numerical solutions obtained with the of Keller-box technique [29,30,31]. The physical features of embedding parameters are discussed through graphs.

2. Formulation

Let us consider a stagnation point flow of an incompressible second grade fluid over a stretching sheet. The stretching and stagnation point is assumed to be of exponential type. The Cartesian coordinates (x, y) are used such that x is along the surface of the sheet, while y is taken normal to it. The related boundary layer equations of second grade fluid in the presence of heat transfer take the following form

$$\frac{\partial u}{\partial x}+\frac{\partial v}{\partial y}=0, \tag{1}$$

$$\begin{aligned} u\frac{\partial u}{\partial x}+v\frac{\partial u}{\partial y} \\ =U_\infty\frac{dU_\infty}{dx}+\upsilon\frac{\partial^2 u}{\partial y^2} \\ +\frac{\alpha_1}{\rho}\left[u\frac{\partial^3 u}{\partial x\partial y^2}+\frac{\partial u}{\partial y}\frac{\partial^2 u}{\partial x\partial y}+v\frac{\partial^3 u}{\partial y^3}+\frac{\partial u}{\partial x}\frac{\partial^2 u}{\partial y^2}\right], \end{aligned} \tag{2}$$

$$u\frac{\partial T}{\partial x}+v\frac{\partial T}{\partial y}=\alpha\frac{\partial^2 T}{\partial y^2}. \tag{3}$$

Here (u,v) are the velocity components along the (x,y) axes, ρ is the fluid density, α_1 is the second grade parameter, ν is the kinematic viscosity, T is temperature, α is the thermal diffusivity, p is pressure and U_∞ is the free-stream velocity. The corresponding boundary conditions for the problem are

$$\text{at} \quad y=0, \quad u=U_w, \quad v=0, \quad T=T_w(x), \tag{4}$$

$$\text{as} \quad y\to\infty, \quad u\to U_\infty, \quad T\to T_\infty, \tag{5}$$

where the free-stream velocity U_∞, the stretching velocity U_w, and the surface temperature T_w, are defined as

$$U_\infty = ae^{x/L}, \quad U_w = be^{x/L}, \quad T_w = T_\infty + ce^{x/L}, \tag{6}$$

in which a and b are constant velocities, c is constant temperature and L is the reference length. Defining the following similarity transformations:

$$u = ae^{x/L} f'(\eta), \quad v = -\left(\frac{\nu a}{2L}\right)^{\frac{1}{2}} e^{x/2L}\left(f(\eta)+\eta f'(\eta)\right), \tag{7}$$

$$\theta = \frac{T-T_\infty}{T_w-T_\infty}, \qquad \eta = \left(\frac{a}{2\nu L}\right)^{\frac{1}{2}} e^{x/2L} y. \tag{8}$$

With the help of transformations defined in *Eqs.* (7) and (8), *Eq.* (1) is identically satisfied and *Eqs.* (2) and (3) take the form

$$f''' + ff'' - 2f'^2 + 2 + \beta\begin{pmatrix} 2\eta f'' f''' + 5 f' f''' \\ +3f''^2 - ff^{iv} \end{pmatrix} = 0, \tag{9}$$

$$\theta'' + \Pr(f\theta' - 2f'\theta) = 0, \tag{10}$$

in which $\beta = \alpha_1 U_\infty / 2\mu L$ is the nondimensional second grade fluid parameter and $\Pr = \nu/\alpha$ is the Prandtl number. The boundary conditions in nondimensional form can be written as

$$f(0)=0, \quad f'(0)=\varepsilon, \quad \theta(0)=1, \tag{11}$$

$$f'\to 1, \quad \theta\to 0, \ \text{as} \ \eta\to\infty, \tag{12}$$

where $\varepsilon = b/a$.

The shear stress on the surfaces τ_w, the frictional drag coefficient C_f, the heat flux at the surface q_w and the local Nusselt numbers Nu in dimensionless form are defined as

$$\tau_w = \frac{1}{\varepsilon^{3/2}}\sqrt{\frac{U_w}{2\nu L}}\left(\mu U_w + \frac{7\alpha_1 U_w^2}{2L}\right) f''(0), \tag{13}$$

$$(\varepsilon \operatorname{Re})^{1/2} C_f = \frac{1}{\varepsilon^2}(\varepsilon + 7\beta) f''(0), \tag{14}$$

$$q_w = -kce^{x/L}\left(\frac{U_w}{2\upsilon L}\right)^{1/2}\theta'(0), \tag{15}$$

$$Nu / \operatorname{Re}_x^{1/2} = -\theta'(0). \tag{16}$$

where $\operatorname{Re} = U_w L / 2\upsilon$, and $\operatorname{Re}_x = U_w x^2 / 2\upsilon L$ is the local Reynolds number.

3. Analytical Solution of the Problem

The analytical solution of the above boundary value problem is obtained with the help of HAM. For HAM solution we choose the initial guesses as

$$f_0(\eta) = (\varepsilon-1) + \eta - (\varepsilon-1)e^{-\eta}, \quad \theta_0(\eta) = e^{-\eta}. \tag{17}$$

The corresponding auxiliary linear operators are

$$L_f = \frac{d^3}{d\eta^3} + \frac{d^2}{d\eta^2}, \qquad L_\theta = \frac{d^2}{d\eta^2} + \frac{d}{d\eta}. \tag{18}$$

They satisfy

$$L_f[c_1 + c_2\eta + c_3 e^{-\eta}] = 0, \quad L_\theta[c_4 + c_5 e^{-\eta}] = 0, \tag{19}$$

where $c_i\ (i=1,\ldots,5)$ are arbitrary constants. The zeroth-order deformation equations are defined as

$$(1-q)L_f[\hat{f}(\eta;q) - f_0(\eta)] = q\hbar_1 N_f[\hat{f}(\eta;q)], \tag{20}$$

$$(1-q)L_\theta[\hat{\theta}(\eta;q) - \theta_0(\eta)] = q\hbar_2 N_\theta[\hat{\theta}(\eta;q)], \tag{21}$$

in which

$$\begin{aligned} N_f[\hat{f}(\eta;q)] = {} & \hat{f}''' + \hat{f}\hat{f}'' - 2\hat{f}'^2 + 2 \\ & + \beta\left(2\eta \hat{f}'' \hat{f}''' + 5\hat{f}'\hat{f}''' + 3\hat{f}''^2 - \hat{f}\hat{f}^{iv}\right), \end{aligned} \tag{22}$$

$$N_\theta[\hat{\theta}(\eta;q)] = \hat{\theta}'' + \Pr(\hat{f}\hat{\theta}' - 2\hat{f}'\hat{\theta}). \tag{23}$$

The appropriate boundary conditions for the zeroth order system are

$$\hat{f}(0;q) = 0, \quad \hat{f}'(0;q) = \varepsilon, \quad \hat{\theta}(0;q) = 1, \tag{24}$$

$$\hat{f}'(\eta;q) \to 1, \quad \hat{\theta}(\eta;q) \to 0, \ \text{as} \ \eta\to\infty. \tag{25}$$

Further details of the HAM solution can be found in [21,22].

4. Numerical Solution

For accuracy of the HAM solution the problem is also solved using the Keller-box technique. For Keller-box scheme the nonlinear system of differential equations is first converted into a first order system using appropriate substitution. This first order system is then approximated by difference equations using central difference. The resulting finite difference system is linearized by applying Newton's method, at the end the obtained linearized system is solved using block-elimination procedure.

5. Results and Discussion

The problem of stagnation point boundary layer flow of a second grade fluid over an exponentially stretching sheet is solved analytically as well as numerically. The analytical solutions of the system of ordinary differential equations $(10-11)$ subject to the boundary conditions $(12-13)$ are obtained through homotopy analysis method (HAM). The convergence of the HAM solution is havily dependent upon the proper selection of $\hbar$'s. To find appropriate values of $\hbar_1$ and $\hbar_2$ the convergence regions of f' and θ are plotted in Figure 1-Figure 3 for specified combinations of involved parameters. Figure 1 is displaying the convergence regions for f for different values of second grade parameter β when stretching parameter $\varepsilon = 0.5$. It is observed that convergence region for viscous fluids $(\beta = 0)$ is $-1 \le \hbar_1 \le 0$ and convergence region is $-0.4 \le \hbar_1 \le 0$ for $\beta = 0$, that is with increase in β convergence region reduced. Figure 2 is graphed for convergence region of f for different values of ε when second grade parameter $\beta = 1$. From Figure 2 it is observed that convergence region for rigid plat case $(\varepsilon = 0)$ is $-0.5 \le \hbar_1 \le 0$, while for $\varepsilon = 2$ convergence region is $-0.13 \le \hbar_1 \le -0.03$. Figure 3 is sketched to observe convergence region for the temperature gradient for specified vales of stretching parameter, second grade parameter and the Prandtl number. It is noted that convergence region is $-1.5 \le \hbar_2 \le -0.3$.

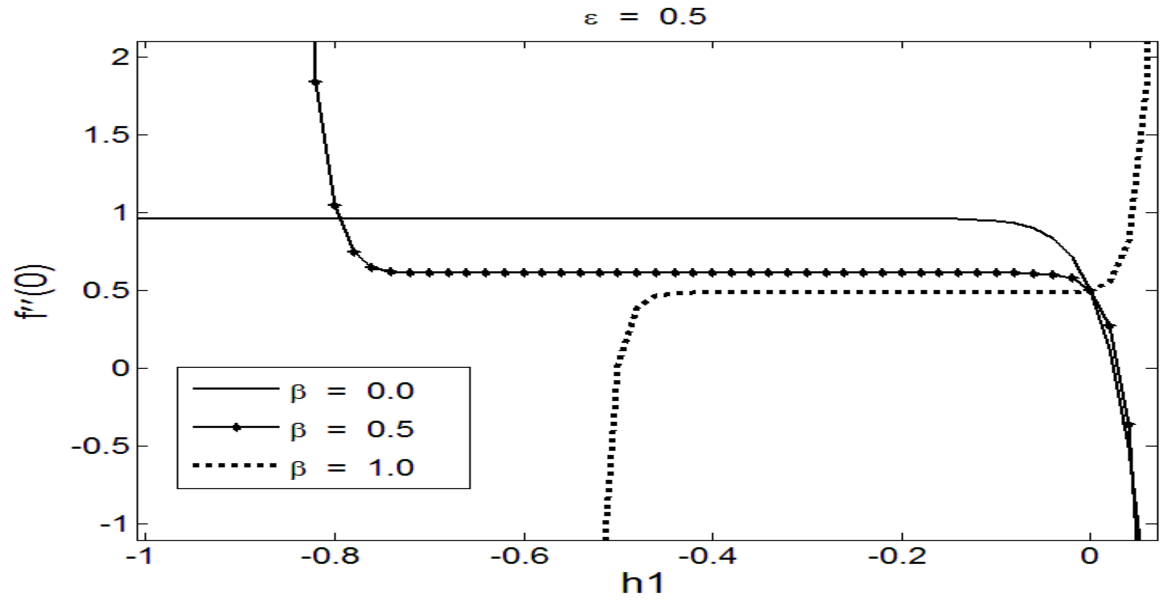

Figure 1. h - curves for f for different β drawn at the 20th order-approximation

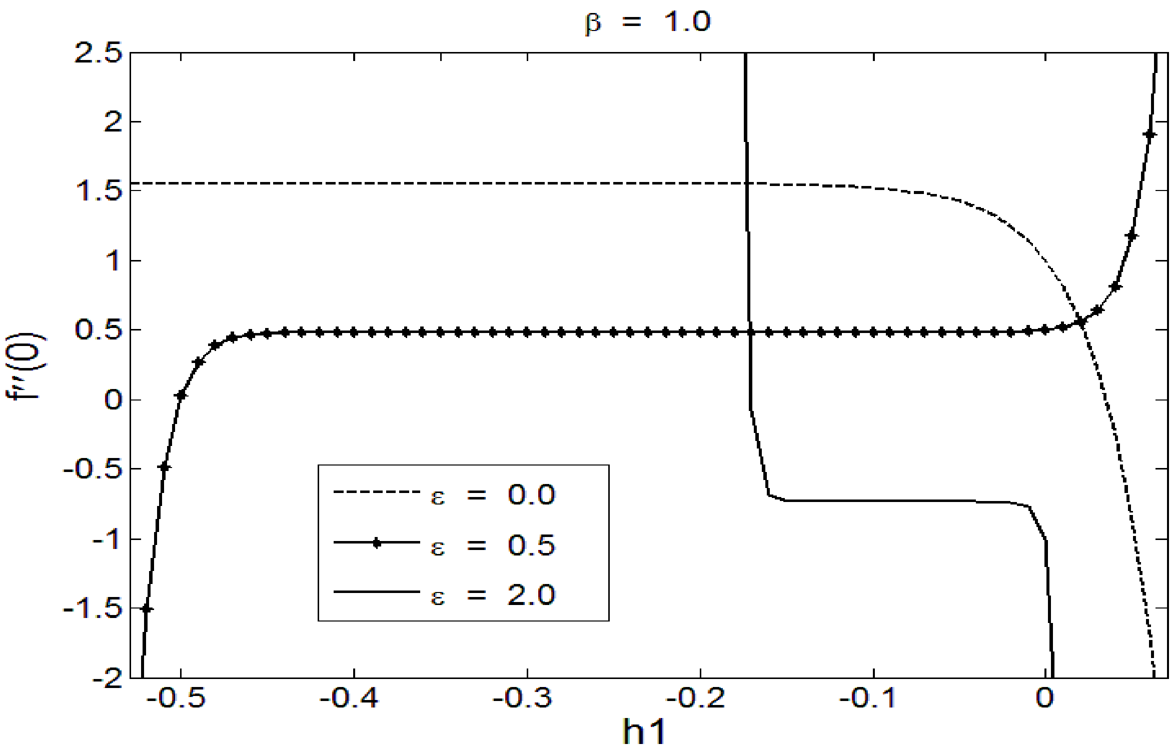

Figure 2. h - curves for f for different ε drawn at the 20th order-approximation

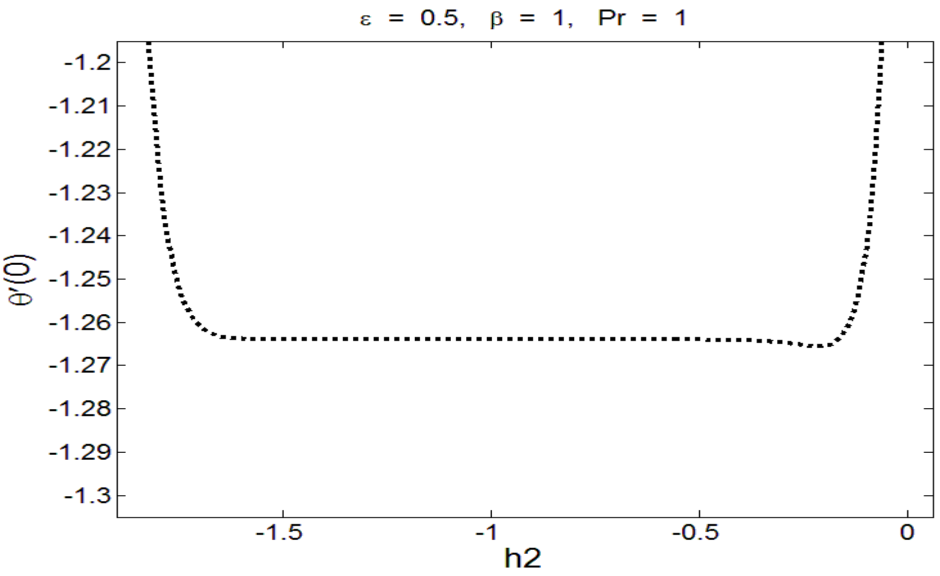

Figure 3. h - curve for θ for different $\Pr$ drawn at the 20th order-approximation

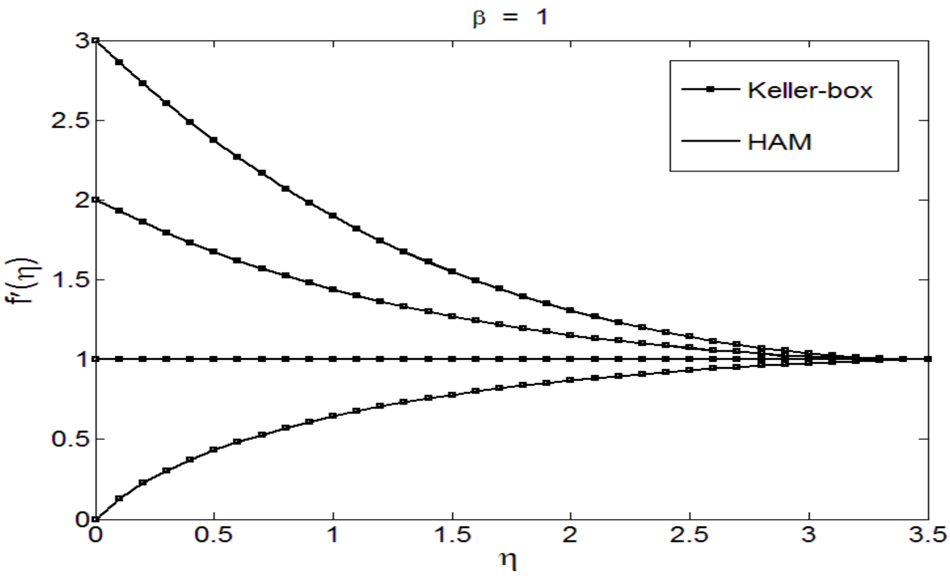

Figure 4. Comparison of Keller-box and HAM solutions for f' for $\varepsilon = 0.0,\ 1.0,\ 2.0,\ 3.0$

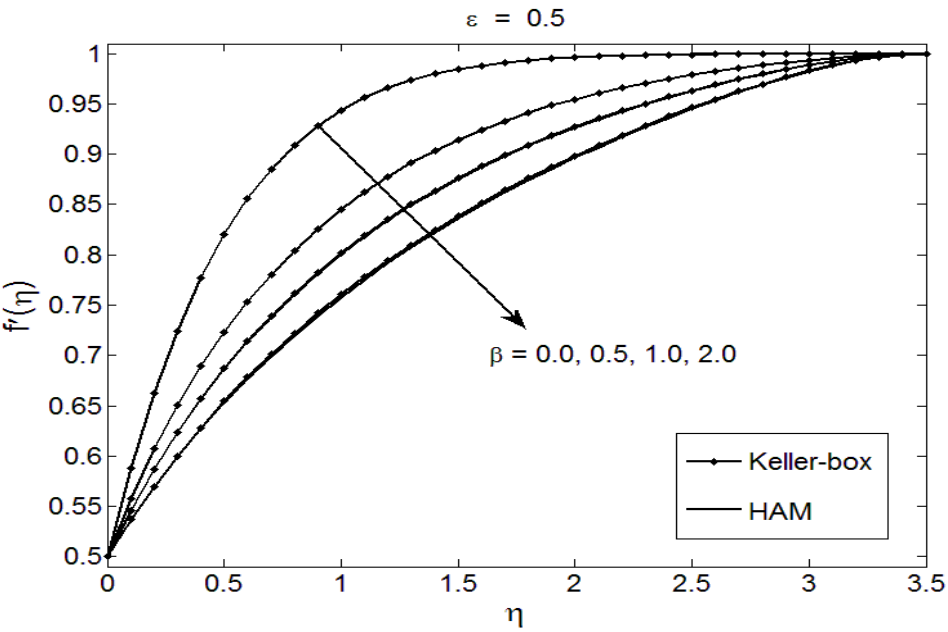

Figure 5. Comparison of Keller-box and HAM solutions for f' for different values of β

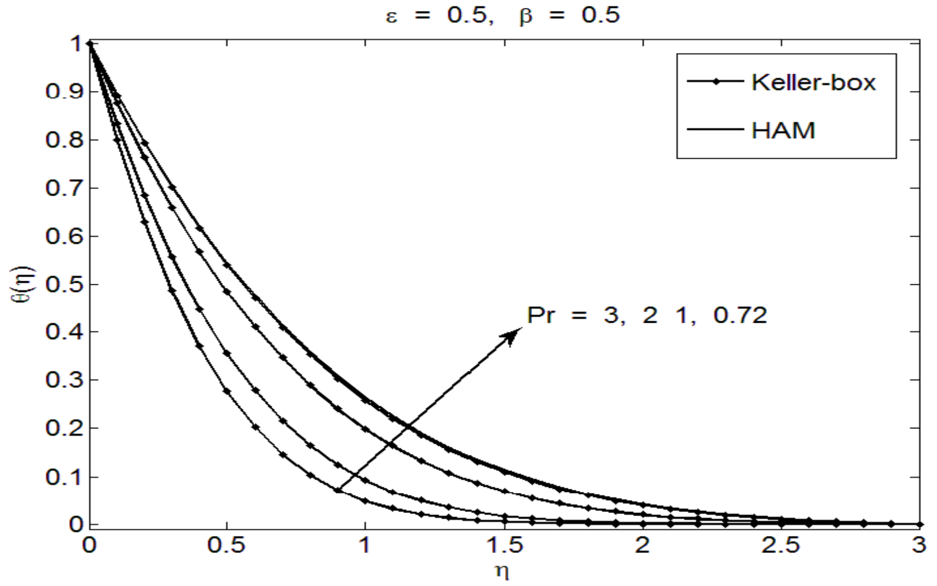

Figure 6. Comparison of Keller-box and HAM solutions for θ for different values of $\Pr$

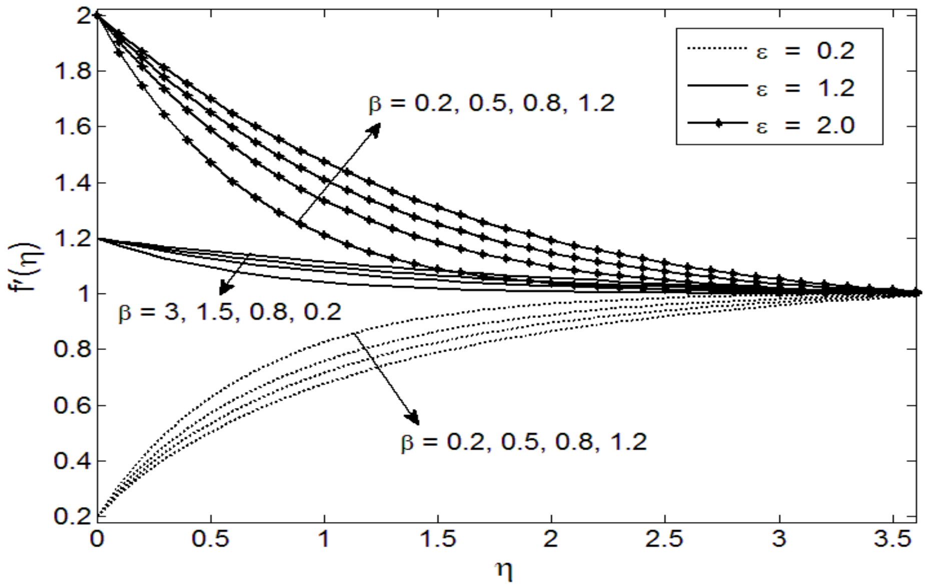

Figure 7. Influence of β over f' for different values of ε

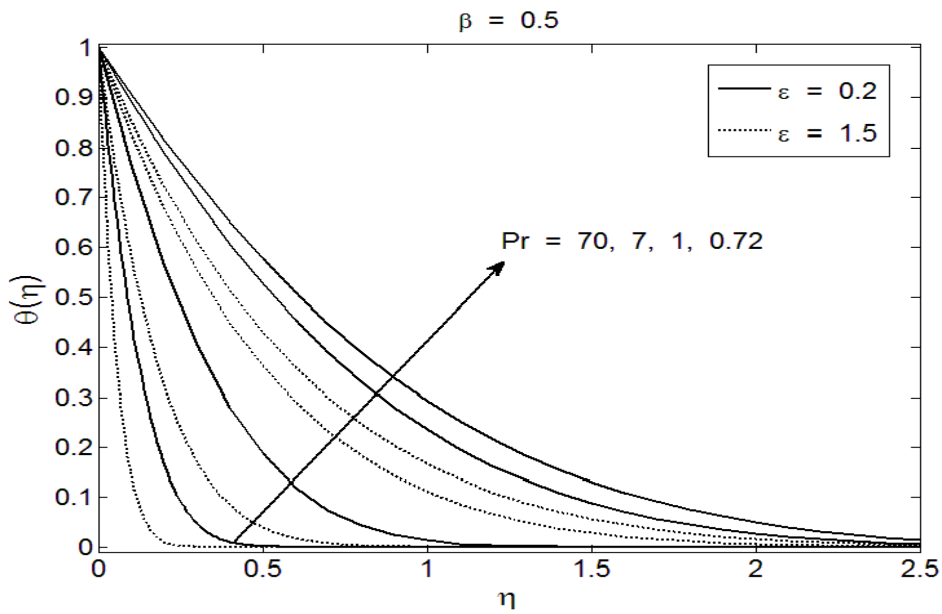

Figure 8. Influence of $\Pr$ over θ for different values of ε

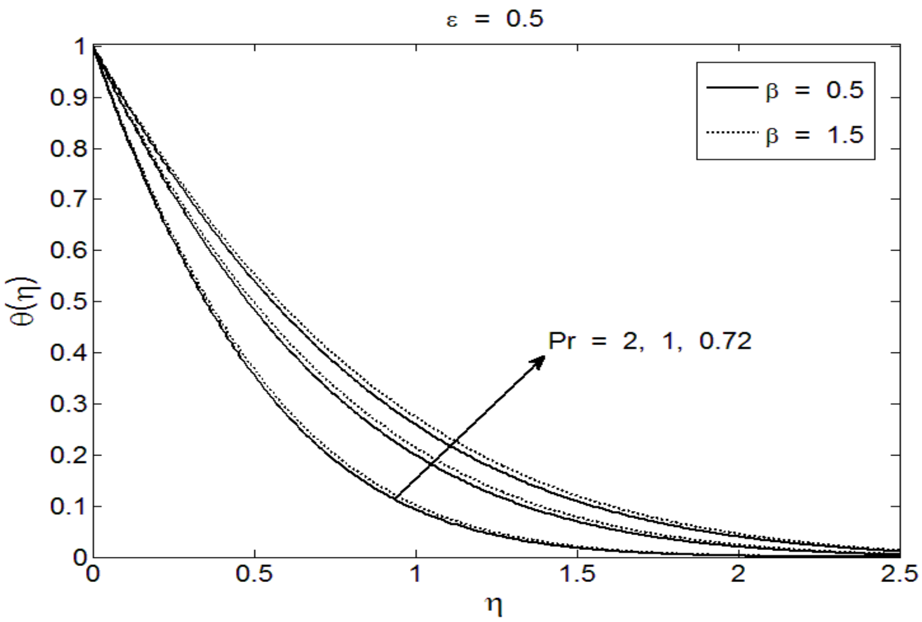

Figure 9. Influence of Pr over θ for different values of β

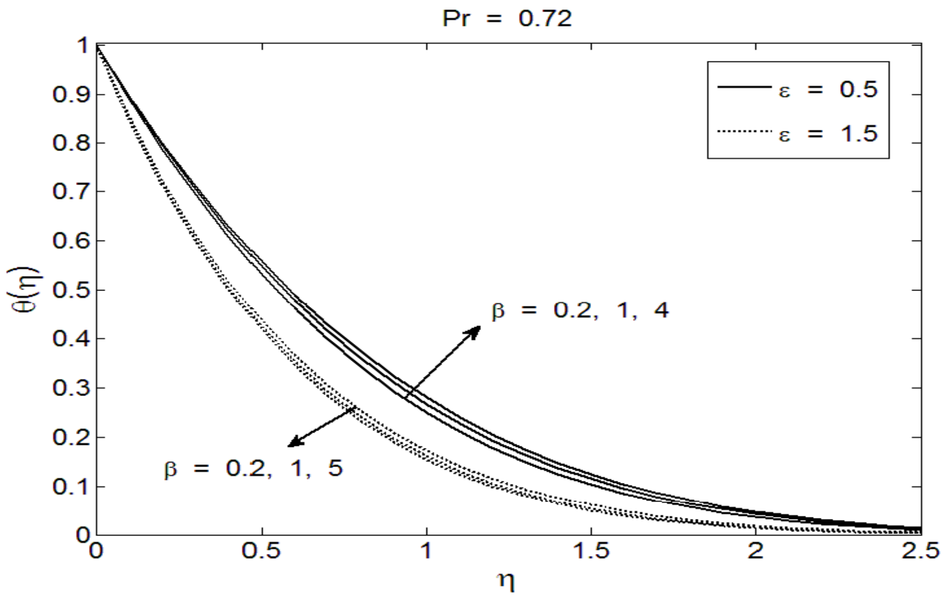

Figure 10. Influence of β over θ for different values of ε

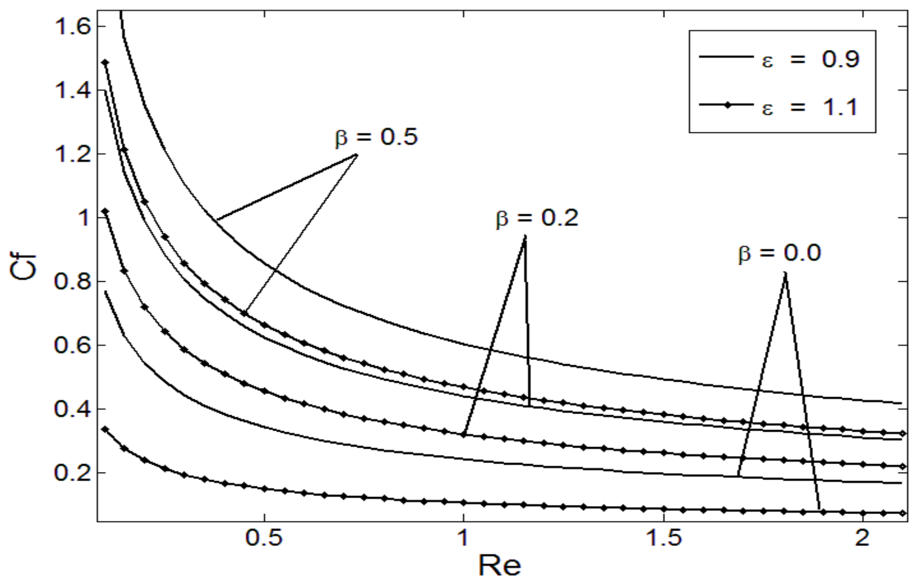

Figure 11. Variation of Skin-friction for different combinations of β and ε against Re

To check accuracy of the HAM solution, the problem is also solved with the help of second order implicit finite difference scheme Keller-box technique. Figure 4-Figure 6 are prepared for comparison of both the HAM and Keller-box solutions for specified values of involved parameters. Figure 4 is schemed to spot behavior of the HAM and Keller-box solutions for different values of ε when $\beta = 1$. It is noted that both solutions are in excellent contract. Figure 5 is organized to observe behavior of the two solutions for different values of second grade parameter β when $\varepsilon = 0.5$. It is witnessed that both the solutions are in decent agreement. From Figure 5 it is also noted that an escalation in second grade parameter β demands a decrease in the velocity profile, this is due to the fact that higher β resembles to higher tensile stress between fluid layers, that in return corresponds to higher resistance to fluid motion. Figure 6 is drawn to check the behavior of the two solutions for the temperature profile θ for different values of the Prandtl number Pr, when $\varepsilon = 0.5$ and $\beta = 0.5$, respectively. From Figure 6 it is seen that both the solutions are again in good agreement and that an increase in Pr demands a decline in the temperature profile θ and also corresponds to decrease in thermal boundary layer thickness. This is due to the fact that large Pr corresponds to low thermal diffusivity, which in return corresponds to less energy transfer ability due to which thermal boundary layer decreases. Figure 7 is designed to observe influence of second grade parameter β over the velocity profile f' for different values of ε. From Figure 7 it is observed that β has a dual behavior for f' for different ε. That is, for $\varepsilon < 1$, an increase in β implies decrease in f', whereas for $\varepsilon > 1$, an increase in β corresponds to a decrease in f'. From Figure 7 it is also noted that f' has greater reliance over β when ε is away from unity, but when ε is near to unity, dependence of f' over β is minimal. Figure 8 is plotted to perceive the effects of Pr for different values of ε. From Figure 8 it is observed that as stretching parameter ε increases the temperature profile decreases more rapidly with respect to Pr, as compare to smaller ε. Figure 9 is drafted to observe the behavior of θ with respect to Pr for different values of second grade parameter β. From Figure 8 it is observed that decrease in θ with Pr is slow for larger values of β. Figure 10 is included to check the behavior of temperature profile against different β when $\varepsilon = 0.5$ and $\varepsilon = 1.5$. It is perceived that θ has a dual behavior against β for different ε, that is when $\varepsilon < 1$, an increase in β produces increase in θ, whereas when $\varepsilon > 1$, an increase in β gives opposite behavior. Figure 11 is affiliated to check behavior of second grade parameter β over skin-friction coefficient against Reynolds number Re for different values of ε. It is depicted from Figure 11 that with an increase in β, skin-friction coefficient increases. The rate of increase in C_f against β decreases with an increase in ε. It is also noted that skin-friction coefficient C_f has strong dependence over ε and behavior of other involved parameters are noticeable only when $\varepsilon \to 1$, whereas, C_f shoots to infinity when $\varepsilon \to 0$, while C_f decays to zero for $\varepsilon >> 1$. Figure 12 portrays behavior of Nusselt numbers Nu for different values of local Reynolds number Re_x against Pr. From Figure 12 an increase is observed in Nu with respect to Re_x.

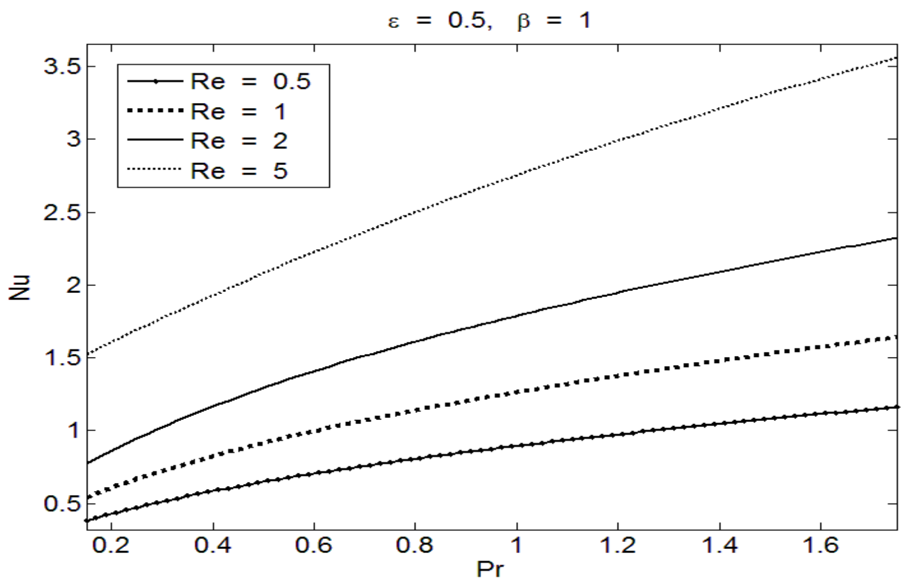

Figure 12. Variation of Nusselt numbers for different values of Re_x against Pr

Table 1-Table 2 are prepared to compare the HAM and Keller-box solutions for velocity and temperature gradients at the surface of stretching sheet. From Table 1-Table 2 it is obvious that both the solutions are compatible. From Table 1 it is also predicted that wall shear stress at the surface τ_w decreases with ε, when $\varepsilon < 1$, while τ_w increases with ε, when $\varepsilon > 1$. Whereas with respect to second grade parameter β wall shear stress τ_w decreases. Table 2 contains values for temperature gradient at surface of stretching sheet. From Table 2 it is noted that with an increase in Pr and ε the local heat flux decreases,

whereas with an increase in β, the heat transfer at the wall decrease.

Table 1. Comparison of behavior of wall shear stress at the surface τ_w, against different parameters. The tabulated values are the corresponding absolute values of $f''(0)$

	f′′(0)							
	HAM	K-b	HAM	K-b	HAM	K-b	HAM	K-b
ε\β	0.0		0.5		1.0		2.0	
0.00	1.6831	1.6831	1.5955	1.5955	1.5531	1.5531	1.5139	1.5139
0.25	1.3354	1.3354	1.0141	1.0141	0.8589	0.8589	0.7103	0.7103
0.50	0.9342	0.9342	0.6147	0.6147	0.4954	0.4954	0.3950	0.3950
0.75	0.4870	0.4870	0.2887	0.2887	0.2270	0.2270	0.1782	0.1782
1.00	0.0000	0.0000	0.0000	0.0000	0.0000	0.0000	0.0000	0.0000
1.25	0.5219	0.5219	0.2669	0.2669	0.2046	0.2046	0.1588	0.1588
1.50	1.0748	1.0748	0.5200	0.5200	0.3959	0.3959	0.3063	0.3063
1.75	1.6554	1.6554	0.7637	0.7637	0.5783	0.5783	0.4469	0.4469
2.00	2.2609	2.2609	1.0009	1.0009	0.7551	0.7551	0.5829	0.5829
3.00	4.8902	4.8902	1.9115	1.9115	1.4287	1.4287	1.1022	1.1022
4.00	7.7774	7.7774	2.7921	2.7921	2.0779	2.0779	1.6043	1.6043
5.00	10.8557	10.8557	3.6595	3.6595	2.7170	2.7170	2.1001	2.1001

Table 2. Comparison of behavior of heat flux at the surface q_w against different parameters

Pr\β		-Θ′(0)							
		HAM	K-b	HAM	K-b	HAM	K-b	HAM	K-b
		0.00		0.50		1.00		2.00	
ε = 0	0.20	0.5750	0.5750	0.5435	0.5435	0.5296	0.5296	0.5163	0.5163
	0.72	0.9209	0.9209	0.8580	0.8580	0.8292	0.8292	0.8012	0.8012
	1.00	1.0436	1.0436	0.9718	0.9718	0.9386	0.9386	0.9061	0.9061
	7.00	2.1405	2.1405	2.0068	2.0068	1.9415	1.9415	1.8755	1.8755
	10.00	2.4351	2.4351	2.2874	2.2874	2.2146	2.2146	2.1407	2.1407
ε = .5	0.20	0.6578	0.6578	0.6351	0.6351	0.6258	0.6258	0.6175	0.6175
	0.72	1.1528	1.1528	1.1079	1.1079	1.0898	1.0898	1.0737	1.0737
	1.00	1.3402	1.3402	1.2891	1.2891	1.2686	1.2686	1.2504	1.2504
	7.00	3.3072	3.3072	3.2160	3.2160	3.1807	3.1807	3.1499	3.1499
	10.00	3.9153	3.9153	3.8160	3.8160	3.7777	3.7777	3.7444	3.7444
ε = 2	0.20	0.8614	0.8614	0.9191	0.9191	0.9361	0.9361	0.9488	0.9488
	0.72	1.7041	1.7041	1.8019	1.8019	1.8268	1.8268	1.8445	1.8445
	1.00	2.0361	2.0361	2.1425	2.1425	2.1686	2.1686	2.1870	2.1870
	7.00	5.7402	5.7402	5.8889	5.8889	5.9207	5.9207	5.9432	5.9432
	10.00	6.9266	6.9266	7.0850	7.0850	7.1185	7.1185	7.1423	7.1423
ε = 3	0.20	0.9765	0.9765	1.0940	1.0940	1.1234	1.1234	1.1444	1.1444
	0.72	2.0061	2.0061	2.1897	2.1897	2.2274	2.2274	2.2531	2.2531
	1.00	2.4129	2.4129	2.6090	2.6090	2.6476	2.6476	2.6738	2.6738
	7.00	6.9659	6.9659	7.2248	7.2248	7.2705	7.2705	7.3014	7.3014
	10.00	8.4306	8.4306	8.7085	8.7085	8.7572	8.7572	8.7903	8.7903

References

[1] M. Y. Malik, M. Naseer, S. Nadeem, Abdul Rehman, The boundary layer flow of Casson nanofluid over a vertical exponentially stretching cylinder, Appl. NanoSci.

[2] M. Y. Malik, M. Naseer, Abdul Rehman, Numerical study of convective heat transfer on the Power Law fluid over a vertical exponentially stretching cylinder, Applied and Computational Mathematics, 4(5), (2015) 346-350.

[3] Abdul Rehman, R. Baza, S. Achakzai, S. Iqbal, M. Naseer, Boundary layer flow and heat transfer of micropolar fluid over a vertical exponentially stretched cylinder, App. Comp. Math. 4(6), (2015), 424-430.

[4] Y. Y. Lok, N. Amin, I. Pop, Non-orthogonal stagnation point flowtowards a stretching sheet, Int. J. Non-Linear Mech. 41 (2006) 622-627.

[5] S. Nadeem, A. Hussain, M. Khan, HAM solutions for boundary layer flow in the region of the stagnation point towards a stretching sheet, Commun. Nonlinear Sci. Numer. Simulat. 15 (2010) 475-481.

[6] M. Naseer, M. Y. Malik, S. Nadeem, Abdul Rehman, The boundary layer flow of hyperbolic tangent fluid over a vertical exponentially stretching cylinder, Alexandria Eng. J. 53(3) (2014), 747-750.

[7] A. Ishak, K. Jafar, R. Nazar, I. Pop, MHD stagnation point flow towards a stretching sheet, Physica A 388 (2009) 3377-3383.

[8] Abdul Rehman, S. Nadeem, M. Y. Malik, Stagnation flow of couple stress nanofluid over an exponentially stretching sheet through a porous medium, J. Power Tech. 93(2) (2013) 122-132.

[9] T. C. Chiam, Heat transfer with variable conductivity in a stagnation-point flow towards a stretching sheet, Int. Comm. Heat Mass Tran. 23 (1996) 239-248.

[10] R. A. V. Gorder, K. Vajravelu, Hydromagnetic stagnation point flow of a second grade fluid over a stretching sheet, Mech. Res. Commun. 37 (2010) 113-118.

[11] Abdul Rehman, S. Nadeem, M. Y. Malik, Boundary layer stagnation-point flow of a third grade fluid over an exponentially stretching sheet, Braz. J. Che. Eng. 30(3) (2013) 611-618.

[12] Abdul Rehman, S. Nadeem, Heat transfer analysis of the boundary layer flow over a vertical exponentially stretching cylinder, Global J. Sci. Fron. Res. 13(11) (2013) 73-85.

[13] T. Fan, H. Xu, I. Pop, Unsteady stagnation flow and heat transfer towards a shrinking sheet, Int. Commun. Heat Mass Tran. 37 (2010) 1440-1446.

[14] S. Nadeem, Abdul Rehman, Axisymmetric stagnation flow of a nanofluid in a moving cylinder, Comp. Math. Mod. 24(2) (2013) 293-306.

[15] S. Nadeem, Abdul Rehman, Mohamed Ali, The boundary layer flow and heat transfer of a nanofluid over a vertical slender cylinder, J. NanoEngineering and NanoSystems (2012) 1-9.

[16] E. Sanjayanad, S. K. Khan, On heat and mass transfer in a viscoelastic boundary layer flow over an exponentially stretching sheet, Int. J. Thermal Sci. 45 (2006) 819-828.

[17] S. K. Khan, E. Sanjayanad,.Viscoelastic boundary layer flow and heat transfer over an exponential stretching sheet, Int. J. Heat Mass Tran. 48 (2005) 1534-1542.

[18] S. Nadeem, S. Zaheer, T. Fang, Effects of thermal radiation on the boundary layer flow of a Jeffrey fluid over an exponentially stretching surface,, Numer. Algor. 57 (2011) 187-205.

[19] S. Nadeem, T. Hayat,M. Y. Malik, S. A. Rajput, Thermal radiation effects on the flow by an exponentially stretching surface: a series solution, Z. Na.. 65 (2010) 495-503

[20] S. Wei. Wong, M. Abu O. Awang, A. Ishak, Stagnation-Point Flow over an Exponentially Shrinking/Stretching Sheet, ZNa. 66a (2011) 705-711.

[21] Sj. Liao, On the homotopy analysis method for nonlinear problems, App. Math. Comp. 147 (2004) 499-513.

[22] Sj. Liao, Beyond Perturbation: Introduction to the Homotopy Analysis Method, Chapman & Hall/CRC Press, Boca Raton, 2003

[23] S. Nadeem, Noreen Sher Akbar, Influence of heat and mass transfer on the peristaltic flow of a Johnson Segalman fluid in a vertical asymmetric channel with induced MHD, J. Taiwan Inst. Che. Eng. 42 (2011) 58-66.

[24] S. Nadeem, Noreen Sher Akbar, Effects of heat and mass transfer peristaltic flow of Williamson fluid in a vertical annulus, Meccanica.

[25] Abdul Rehman, S. Nadeem, Mixed convection heat transfer in micropolar nanofluid over a vertical slender cylinder, Chin. Phy. Lett. 29 (12) (2012) 124701-5.

[26] S. Nadeem, Abdul Rehman, Changhoon Lee, Jinho Lee, Boundary layer flow of second grade fluid in a cylinder with heat transfer, Mathematical Problems in Engineering, Volume 2012, Article ID 640289.

[27] L. Zou, Z. Zong, G. H. Dong, Generalizing homotopy analysis method to solve Lotka--Volterra equation, Comp Math App 56 (2008) 2289-2293.

[28] S. Nadeem, Abdul Rehman, K. Vajravelu, Jinho Lee, Changhoon Lee, Axisymmetric stagnation flow of a micropolar nanofluid in a moving cylinder, Mathematical Problems in Engineering, Volume 2012, Article ID 378259.

[29] H. B. Keller, T. Cebeci, Accurate numerical methods for boundary-layer flows. II: Two-dimensional flows, AIAA Journal 10 (1972) 1193-1199.

[30] M. Abramowitz, Stegun IA (1965) Handbook of mathematical functions, Dover, New York.

[31] F. Aman, A. Ishak, Hydromagnetic flow and heat transfer adjacent to a stretching vertical sheet with prescribed surface heat flux, Heat Mass Transfer, 46 (2010) 61-620.